**Group meeting**
19 Jan. 2011
*Amir Feizpour*

# Optomechanically Induced Transparency

# Optomechanically Induced Transparency

**Stefan Weis,[1,2]* Rémi Rivière,[2]* Samuel Deléglise,[1,2]* Emanuel Gavartin,[1] Olivier Arcizet,[3]**
**Albert Schliesser,[1,2] Tobias J. Kippenberg[1,2]†**

a control field $\overline{a}e^{-i\omega_1 t}$, containing $|\overline{a}|^2$photons, in the cavity. The static radiation pressure originating from this field displaces the mechanical mode by $\overline{x}$, leading to an effective detuning from the cavity resonance $\overline{\Delta} = \omega_1 - (\omega_c + G\overline{x})$. We consider the situation where the control laser is

2010

Electromag
and molecu
field. We c
an optical
optomecha
field, indu
transparen
optomecha

C ohe
mu

# Supporting Online Material for Optomechanically induced transparency

Stefan Weis[1,2,†], Rémi Rivière[2,†], Samuel Deléglise[1,2,†], Emanuel Gavartin[1],
Olivier Arcizet[3], Albert Schliesser[1,2], Tobias J. Kippenberg[1*]

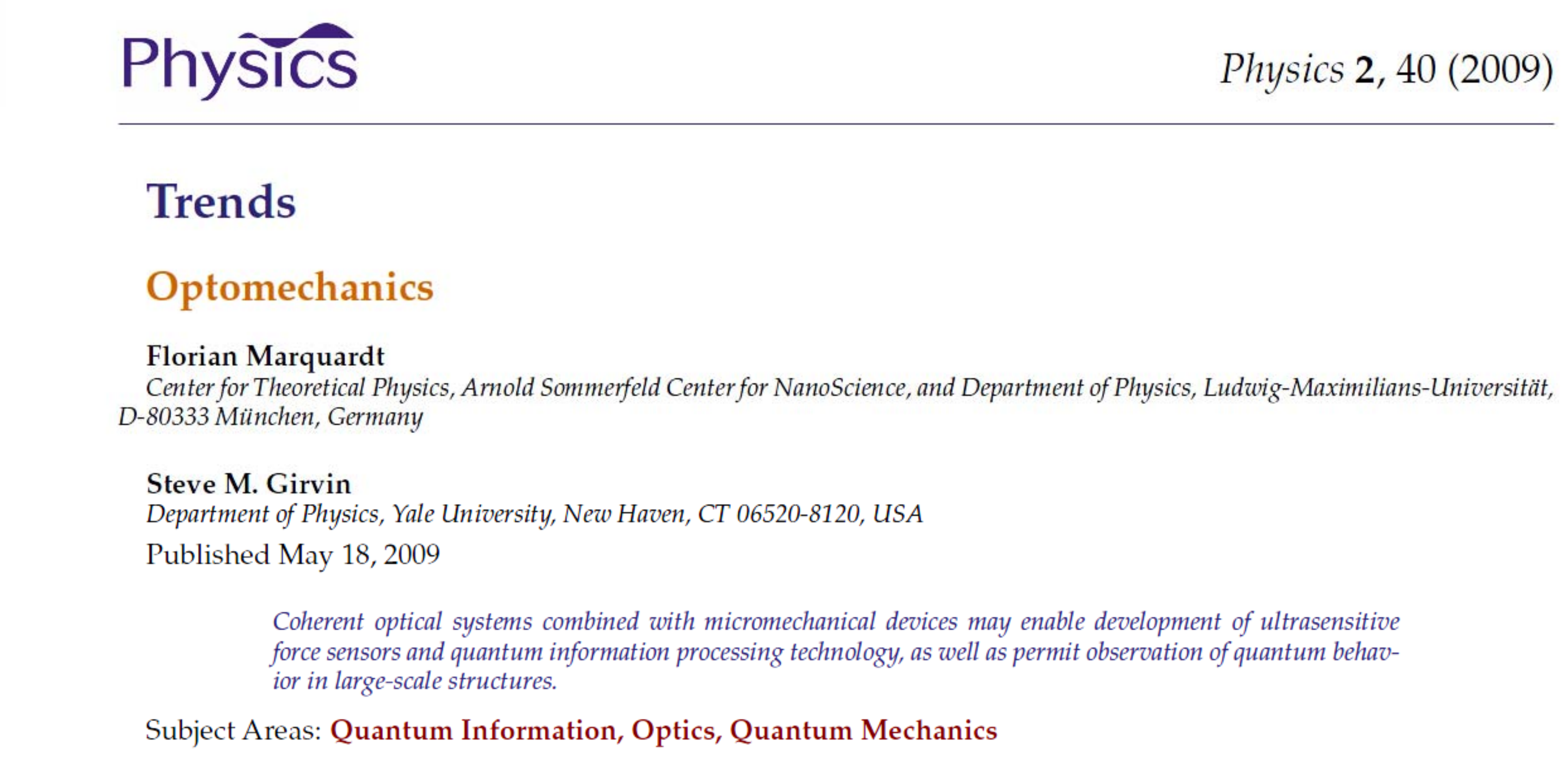

Physics

*Physics* **2**, 40 (2009)

## Trends

# Optomechanics

**Florian Marquardt**
*Center for Theoretical Physics, Arnold Sommerfeld Center for NanoScience, and Department of Physics, Ludwig-Maximilians-Universität, D-80333 München, Germany*

**Steve M. Girvin**
*Department of Physics, Yale University, New Haven, CT 06520-8120, USA*

Published May 18, 2009

*Coherent optical systems combined with micromechanical devices may enable development of ultrasensitive force sensors and quantum information processing technology, as well as permit observation of quantum behavior in large-scale structures.*

Subject Areas: **Quantum Information, Optics, Quantum Mechanics**

# Outline

- Introduction
  - Optomechanics
  - Induced Transparency
- OMIT
  - Concept
  - Experiment
  - Results
- Summary and conculsions

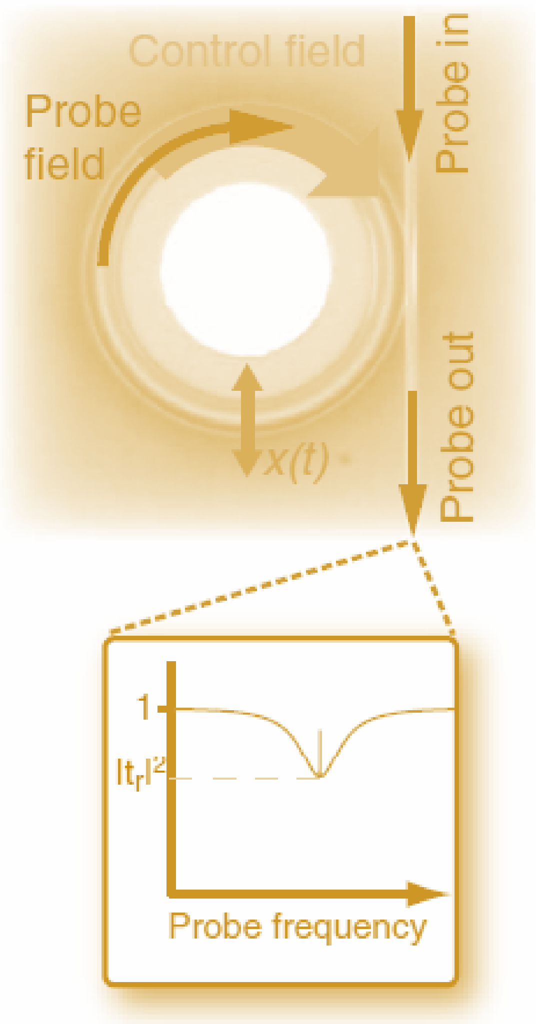

# Optomechanics

- Basic principle: EM radiation can exert force on material objects: *eg.* reflecting light
- Uses: to cool objects or to amplify small forces
  - The gradient of the force adds to the spring constant
- Examples
  - (macroscopic mirrors in) LIGO, Vibrating micro-cavities, Cold Atoms
  - Cooling a mechanical system to its quantum ground state is a key goal of the new field of optomechanics.
  - To get rid of the back-action in optical measurement of position

# Optomechanics *(cnt'd)*

Cooling

fication

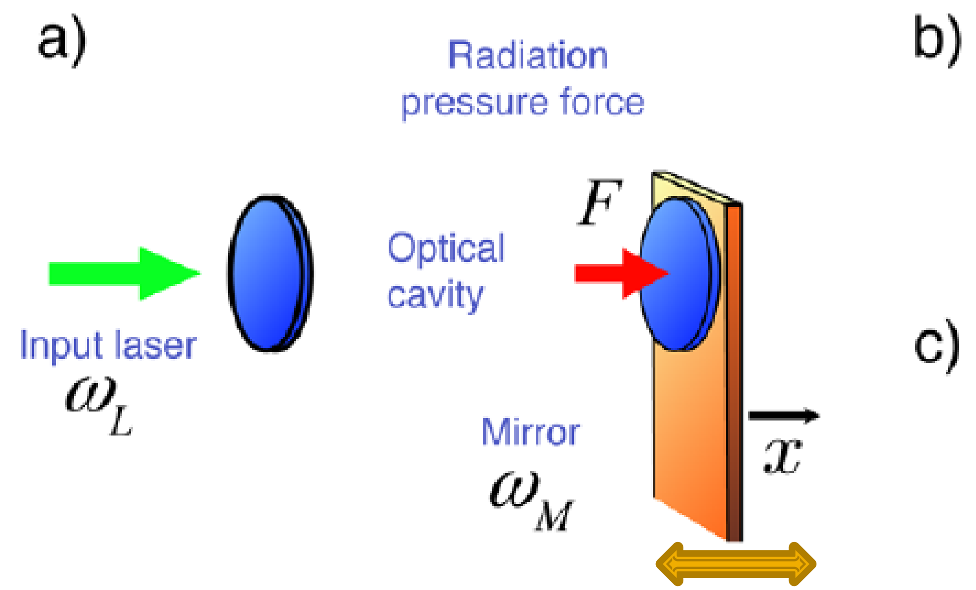

. domain
ure of cooling
I and PM)

Thermal fluctuation or
Radiation pressure

FIG. 1: (a) Schematic optomechanical setup. An optical cavity

# Optomechanics *(cnt'd)*

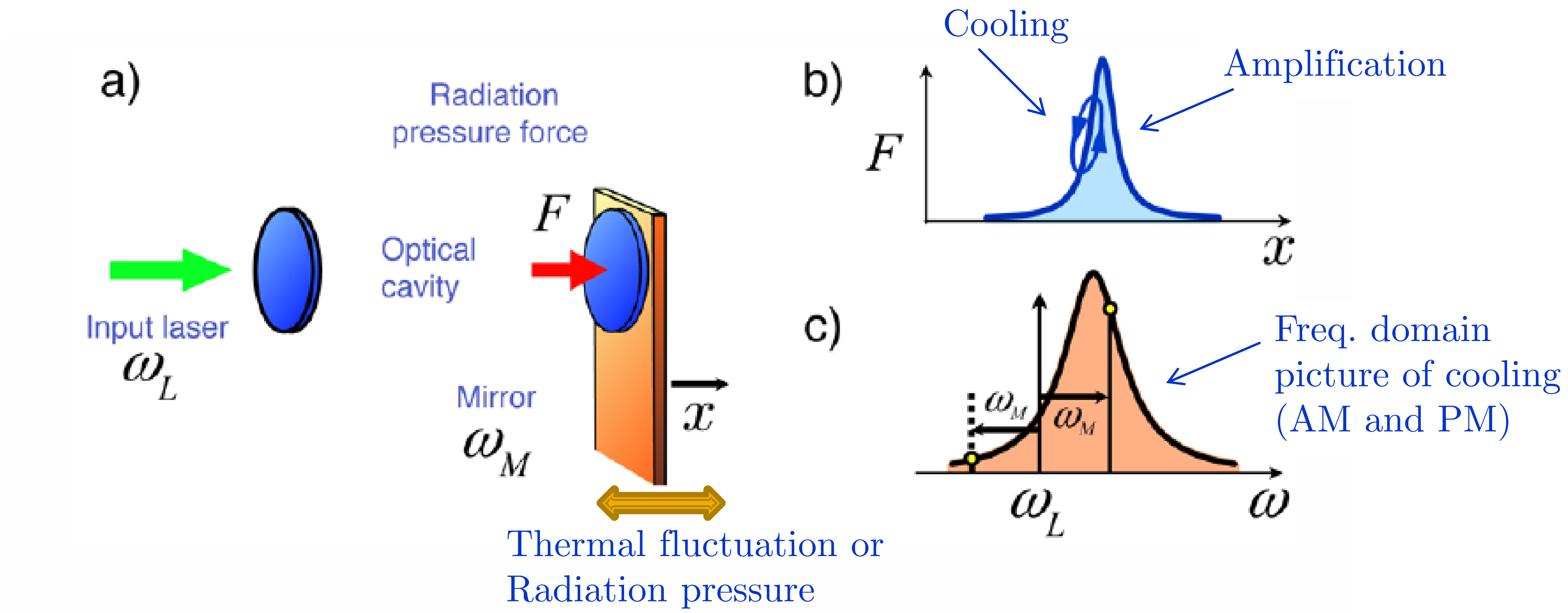

Cooling

Amplification

Freq. domain picture of cooling (AM and PM)

Thermal fluctuation or Radiation pressure

FIG. 1: (a) Schematic optomechanical setup. An optical cavity

The radiation force on the cavity mirror is "viscous" due to a time lag in response of the cavity (ring-down time, here).

$$T_{\text{eff}} = T\Gamma/(\Gamma + \Gamma_{\text{opt}})$$

# Optomechanics *(cnt'd)*

- On the most general level, we are dealing with a resonance (the optical cavity mode) that is driven (by a laser), and whose resonance frequency is pulled by the displacement of some mechanical degree of freedom (the movable mirror).
  - The system can be cold atoms, superconducting circuits, LIGO mirrors, etc.

# Induced transparency

- ???

# OMIT

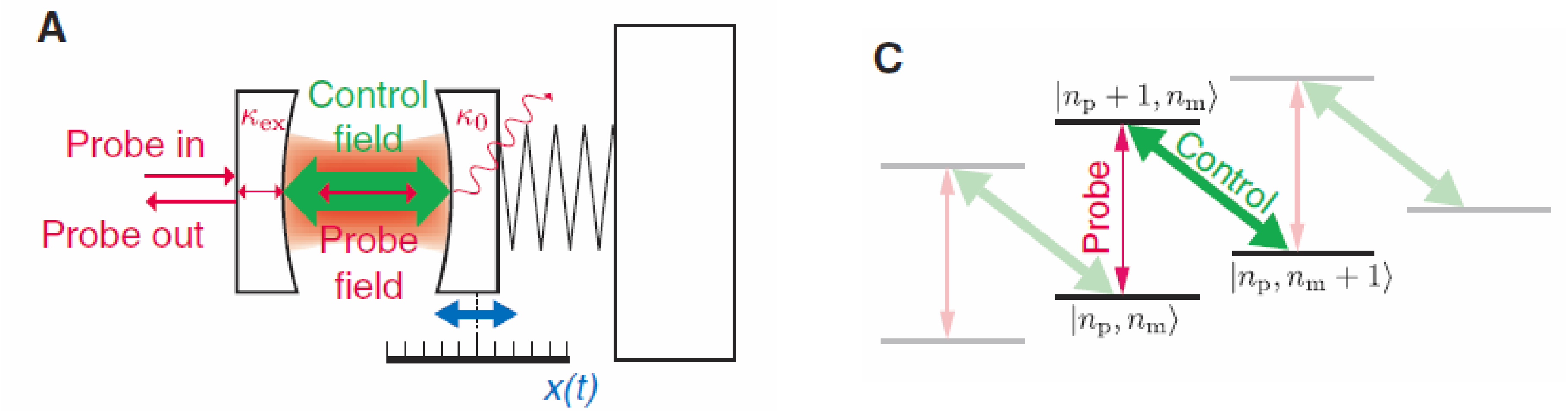

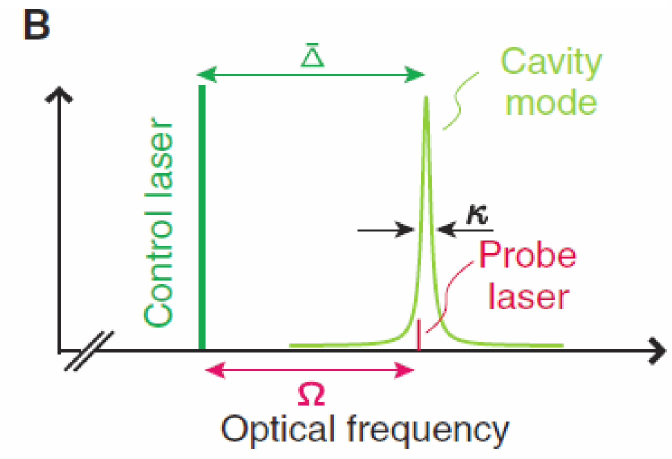

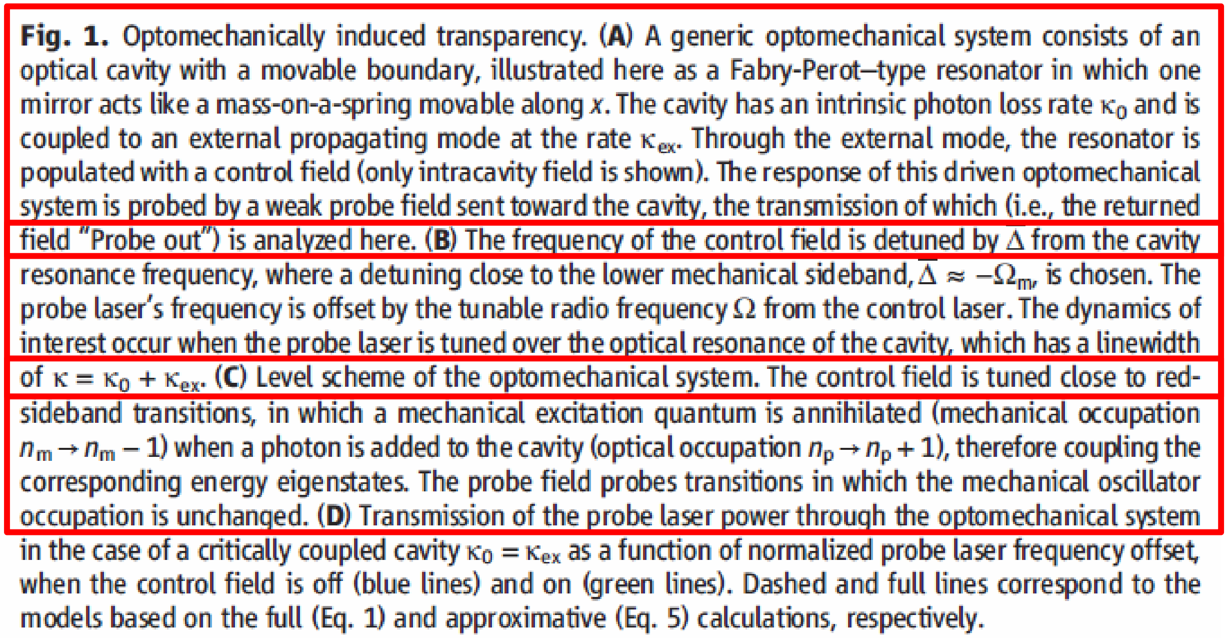

**Fig. 1.** Optomechanically induced transparency. (**A**) A generic optomechanical system consists of an optical cavity with a movable boundary, illustrated here as a Fabry-Perot–type resonator in which one mirror acts like a mass-on-a-spring movable along $x$. The cavity has an intrinsic photon loss rate $\kappa_0$ and is coupled to an external propagating mode at the rate $\kappa_{ex}$. Through the external mode, the resonator is populated with a control field (only intracavity field is shown). The response of this driven optomechanical system is probed by a weak probe field sent toward the cavity, the transmission of which (i.e., the returned field "Probe out") is analyzed here. (**B**) The frequency of the control field is detuned by $\bar{\Delta}$ from the cavity resonance frequency, where a detuning close to the lower mechanical sideband, $\bar{\Delta} \approx -\Omega_m$, is chosen. The probe laser's frequency is offset by the tunable radio frequency $\Omega$ from the control laser. The dynamics of interest occur when the probe laser is tuned over the optical resonance of the cavity, which has a linewidth of $\kappa = \kappa_0 + \kappa_{ex}$. (**C**) Level scheme of the optomechanical system. The control field is tuned close to red-sideband transitions, in which a mechanical excitation quantum is annihilated (mechanical occupation $n_m \rightarrow n_m - 1$) when a photon is added to the cavity (optical occupation $n_p \rightarrow n_p + 1$), therefore coupling the corresponding energy eigenstates. The probe field probes transitions in which the mechanical oscillator occupation is unchanged. (**D**) Transmission of the probe laser power through the optomechanical system in the case of a critically coupled cavity $\kappa_0 = \kappa_{ex}$ as a function of normalized probe laser frequency offset, when the control field is off (blue lines) and on (green lines). Dashed and full lines correspond to the models based on the full (Eq. 1) and approximative (Eq. 5) calculations, respectively.

# OMIT

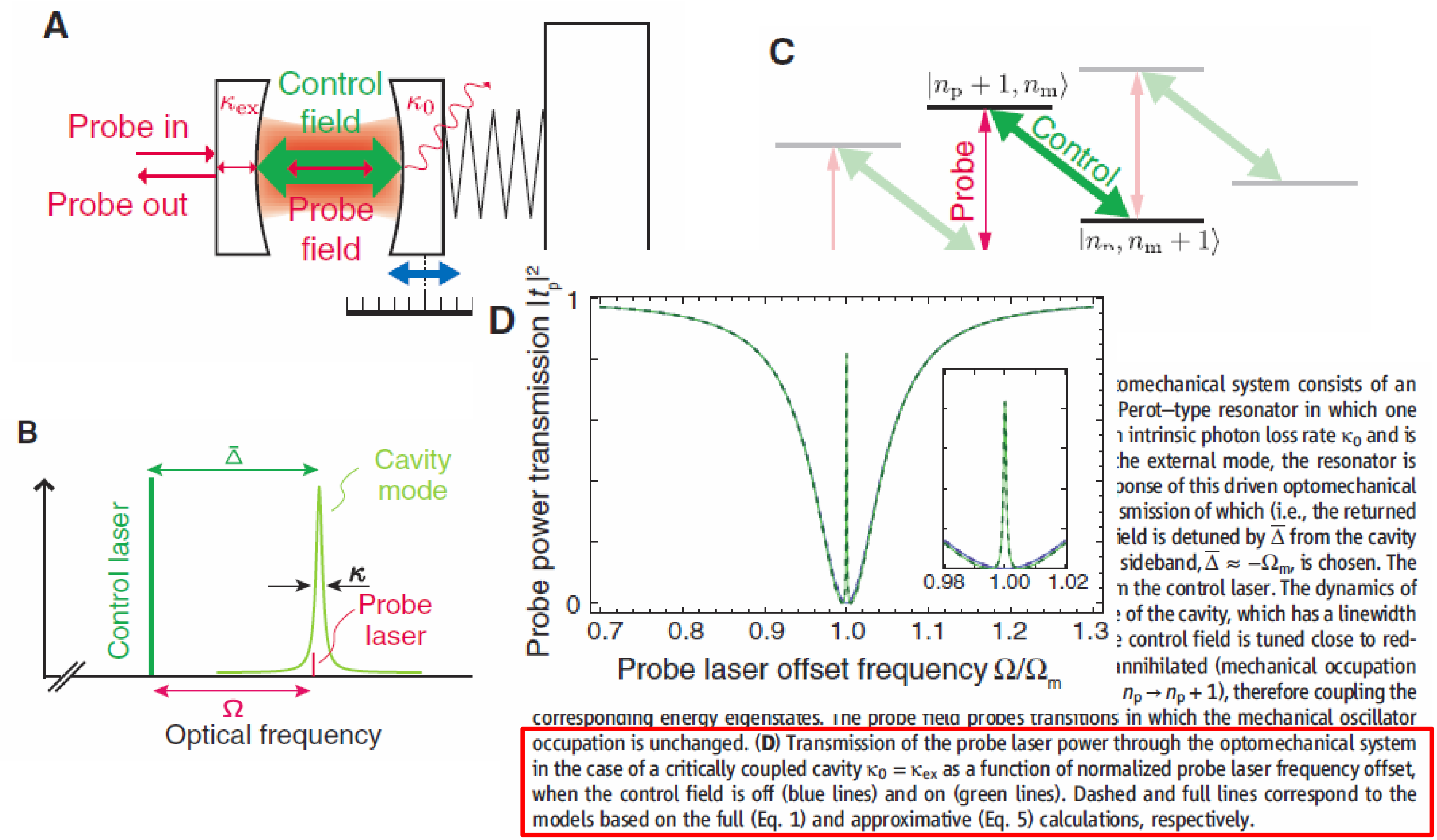

omechanical system consists of an
Perot–type resonator in which one
intrinsic photon loss rate $\kappa_0$ and is
he external mode, the resonator is
ponse of this driven optomechanical
smission of which (i.e., the returned
ield is detuned by $\bar{\Delta}$ from the cavity
sideband, $\bar{\Delta} \approx -\Omega_m$, is chosen. The
n the control laser. The dynamics of
of the cavity, which has a linewidth
control field is tuned close to red-
nnihilated (mechanical occupation
$n_p \rightarrow n_p + 1$), therefore coupling the
corresponding energy eigenstates. The probe field probes transitions in which the mechanical oscillator occupation is unchanged. **(D)** Transmission of the probe laser power through the optomechanical system in the case of a critically coupled cavity $\kappa_0 = \kappa_{ex}$ as a function of normalized probe laser frequency offset, when the control field is off (blue lines) and on (green lines). Dashed and full lines correspond to the models based on the full (Eq. 1) and approximative (Eq. 5) calculations, respectively.

# OMIT *(cnt'd)*

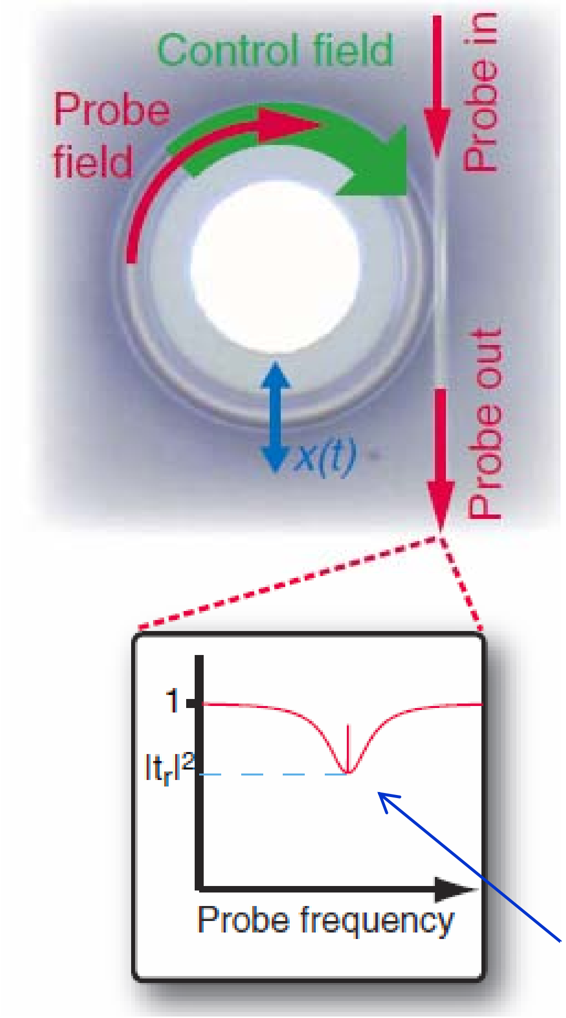

**Fig. 2.** Optomechanical system. (**Top**) A toroidal microcavity is used to demonstrate OMIT: The resonator is coupled to the control and probe fields using a tapered fiber. The optical mode couples through radiation pressure force to the mechanical radial breathing mode of the structure. In this ring geometry, the cavity transmission, defined by the ratio of the returned probe-field amplitude divided by the incoming probe field is simply given by the transmission through the tapered fiber. (**Bottom**) Under the chosen waveguide-toroid coupling conditions, there is a nonzero probe power transmission $|t_r|^2$ at resonance. The control field induces an additional transparency window with a contrast up to $1 - |t_r|^2$.

- Under-coupled (loss rate is more than coupling rate)
- Chance of populating CCW mode

# Experiment

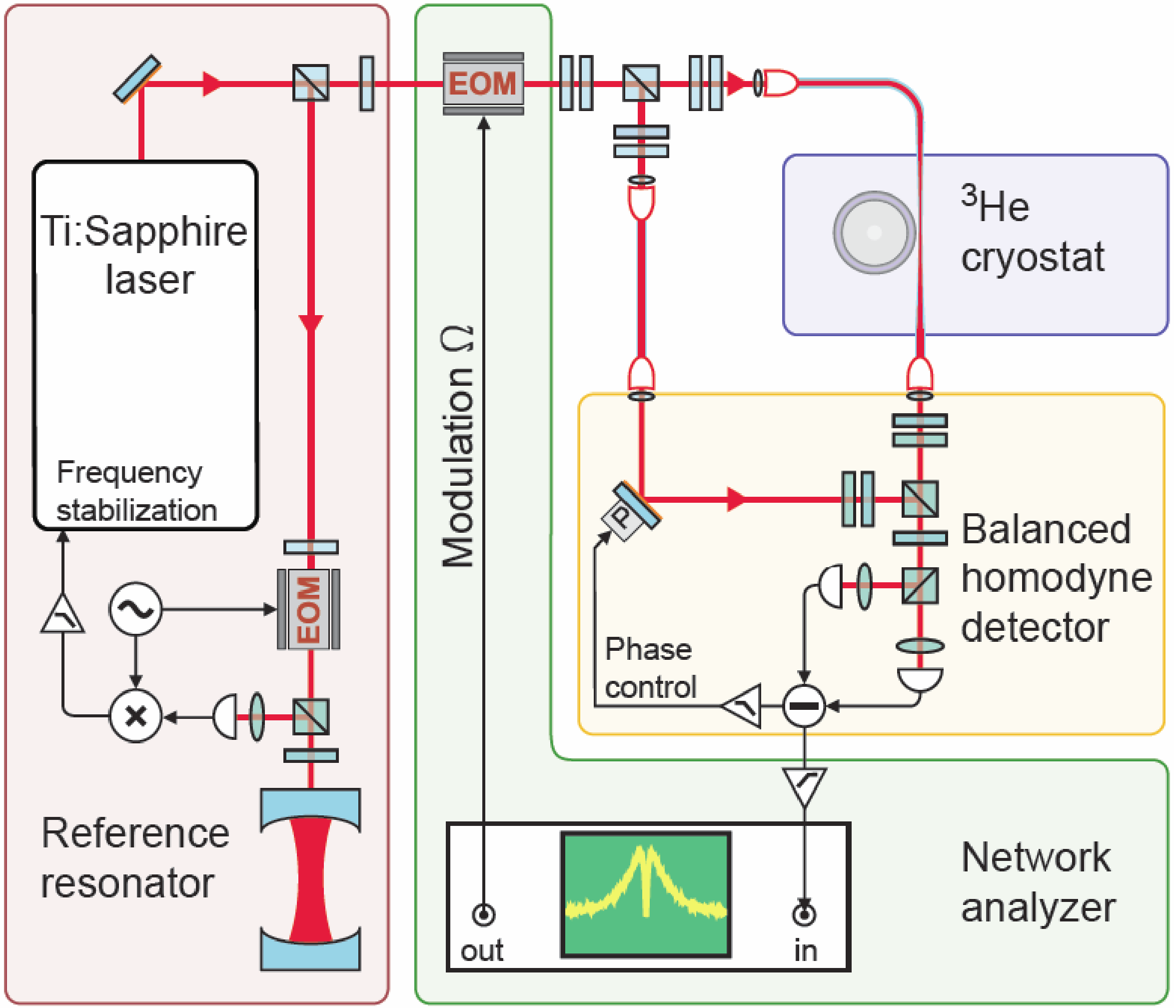

**Figure S1:** Experimental setup. An optomechanical system consisting of a toroid micro-resonator held at cryogenic temperatures in a Helium-3 buffer gas cryostat. The control and probe fields are derived from a single Ti:sapphire laser, which is stabilized to an external reference resonator using the Pound-Drever-Hall technique. While the laser carrier is used as control beam, the probe beam is created by a phase modulator driven at the radio frequency. This optical input is split into two arms, one of which is sent to a tapered fiber in the cryostat, which allows optical coupling to the whispering gallery mode of the toroidal resonator as shown in micrograph with a 60 um-diameter toroid. The other arm serves as the local oscillator in a balanced homodyne receiver used to analyze the light returned from the optomechanical system. While the receiver's DC component is used to lock the phase of the local oscillator, the AC component is analyzed using a network analyzer.

# Experiment *(cnt'd)*

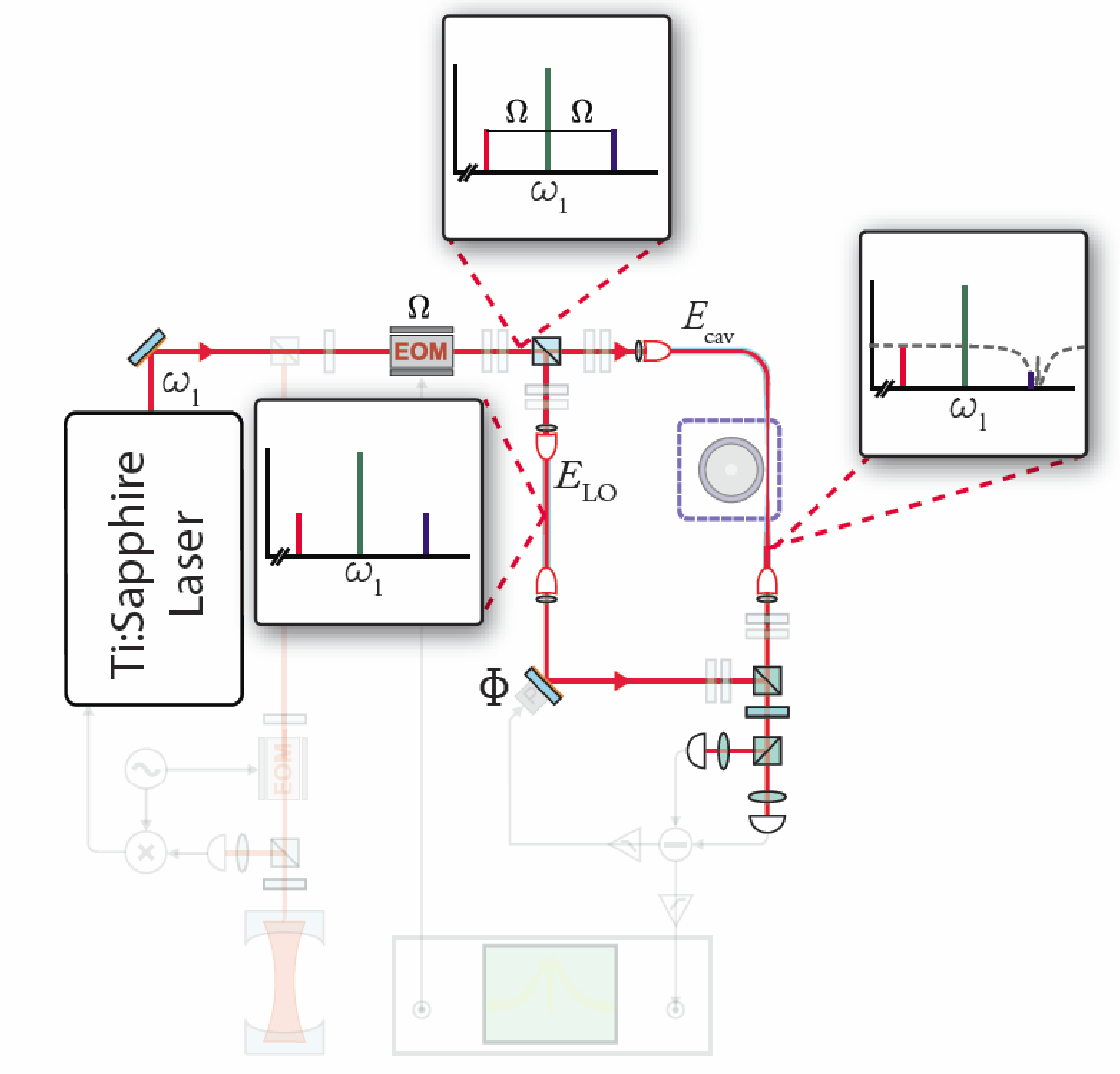

**Figure S2**: The optical setup as described in Figure S1. The laser is phase modulated, creating two sidebands at frequency Ω. The local oscillator field is transmitted unchanged whereas the field in the signal arm is affected by the cavity transmission. In the RSB regime, lower sideband and carrier, off resonant by approximately 2Ω_m and Ω_m are not affected.

# Results

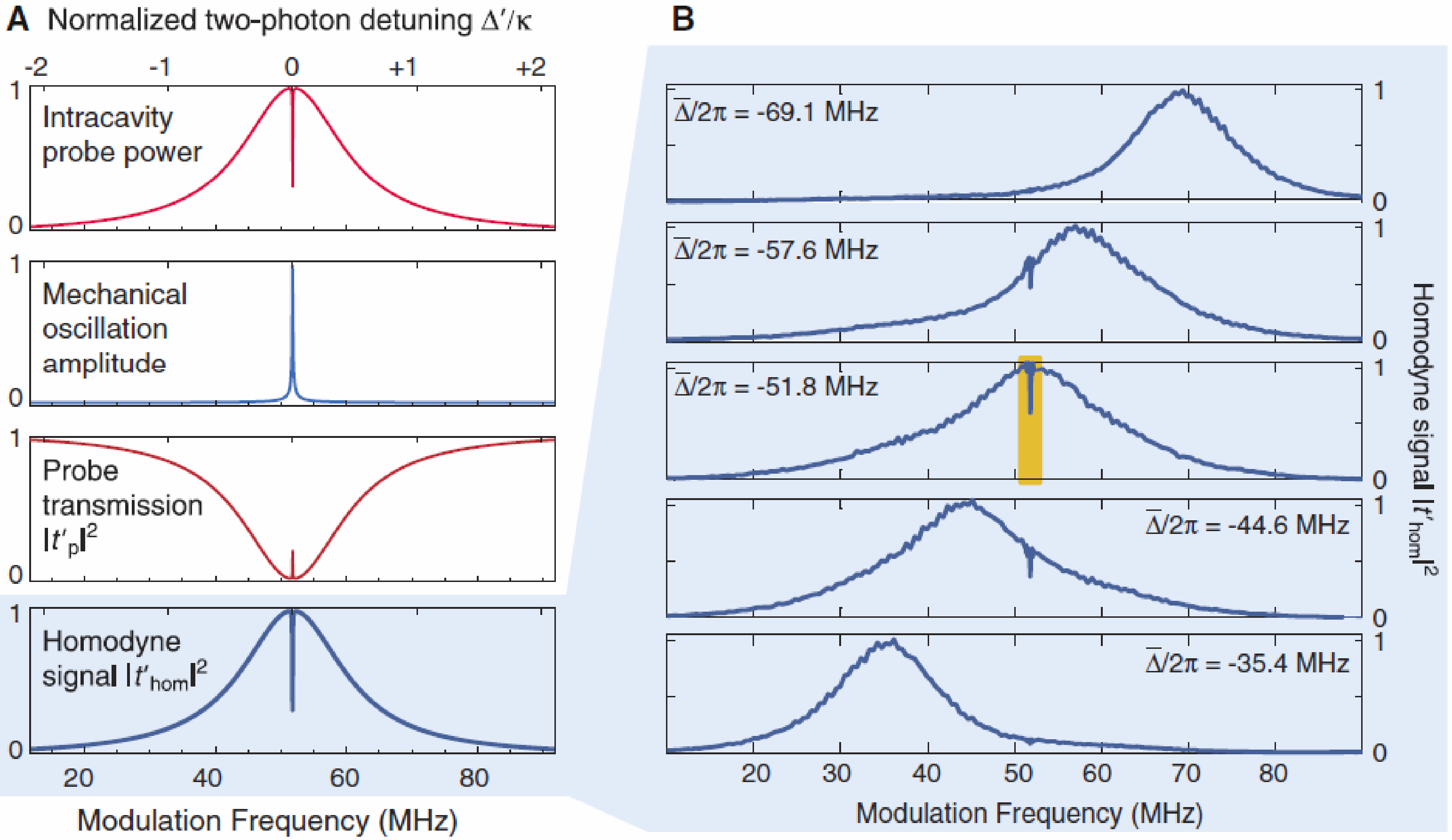

**Fig. 3.** Observation of OMIT. (**A**) Theoretically expected intracavity probe power, oscillation amplitude *X*, normalized probe power transmission $|t'_p|^2$, and the normalized homodyne signal $|t'_{hom}|^2$ as a function of the modulation frequency $\Omega/2\pi$ (top to bottom panels). The first two panels have additionally been normalized to unity. When the two-photon resonance condition $\Delta' = 0$ is met, the mechanical oscillator is excited, giving rise to destructive interference of excitation pathways for an intracavity probe field. The probe transmission therefore exhibits an inverted dip, which can be easily identified in the homodyne signal. (**B**) Experimentally observed normalized homodyne traces when the probe frequency is scanned by sweeping the phase modulator frequency $\Omega$ for different values of control beam detuning $\bar{\Delta}$. Whereas the center of the response of the bare optical cavity shifts correspondingly, the sharp dip characteristic of OMIT occurs always for $\Delta' = 0$. The power of the control beam sent to the cavity is 0.5 mW in these measurements. The middle panel shows the operating conditions where the control beam is tuned to the lower motional sideband $\bar{\Delta} \approx -\Omega_m = -2\pi \cdot 51.8$ MHz. The region around the central dip (orange background) is studied in more detail in a dedicated experimental series (see Fig. 4).

# Results *(cnt'd)*

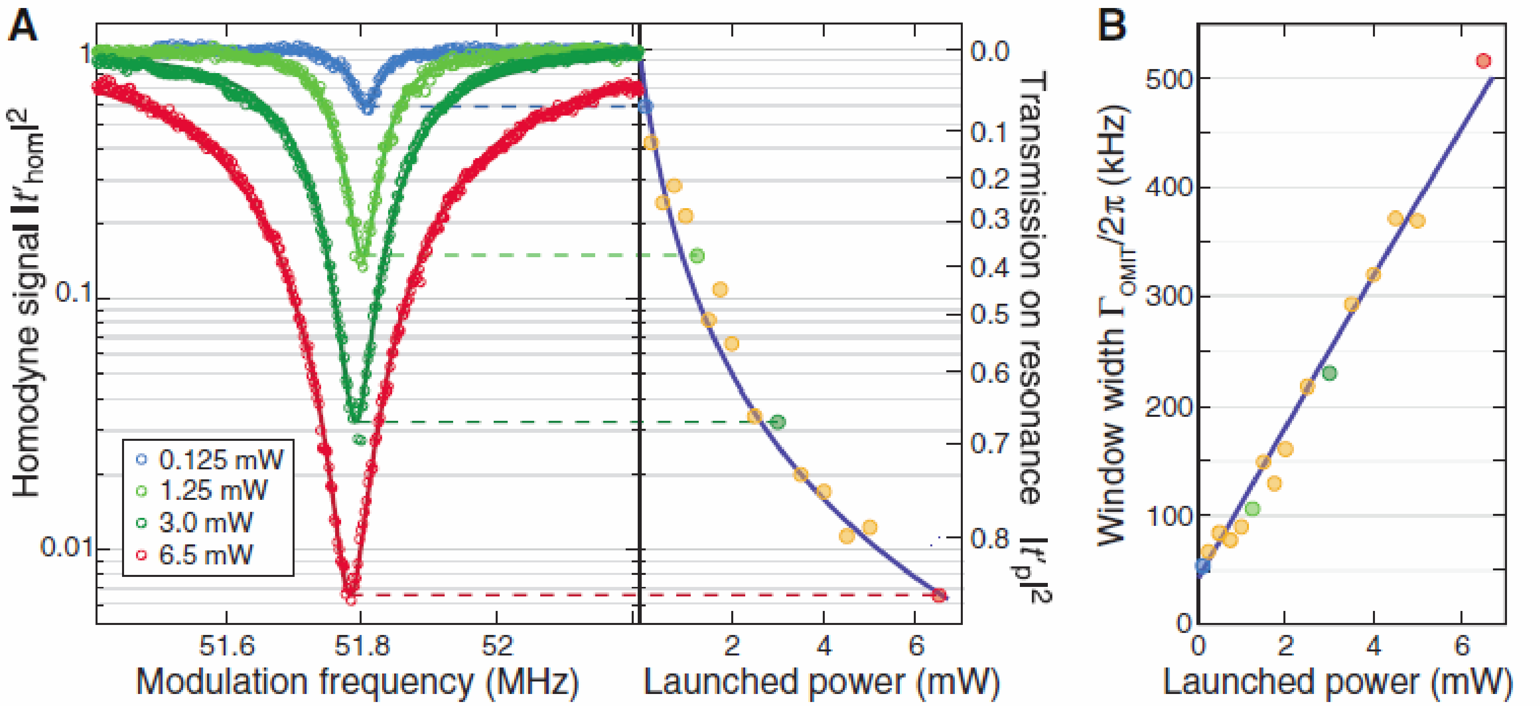

**Fig. 4.** Controlling OMIT. (**A**) Experimental normalized homodyne traces in the presence of a control beam (circles) for four different powers in the control beam from 0.125 mW up to 6.5 mW, and Lorentzian models. The minimum homodyne signal (measured at $\Delta' = 0$) directly indicates the maximum probe power transmission achieved in this case. These values are given in the right panel for a larger set of probe scans, together with the theoretical model developed in this work. (**B**) Width of the transparency window extracted from the same set of probe scans. Good agreement with the theoretical prediction is found over the entire power range.

$$\Omega_c = 2\bar{a}Gx_{zpf}$$

$$x_{zpf} = \sqrt{\hbar/2m_{eff}\Omega_m}$$

$$\Gamma_{OMIT} \approx \Gamma_m(1+C)$$

$$t'_p(\Delta'=0) = C/(C+1)$$

$$C \equiv \Omega_c^2/\Gamma_m\kappa$$

# Conclusions

- Controllable induced transparency
- Telecom wavelength
- All-optical switching (~1000 control photons)
- Different from cooling